



Ultrastructural variability of mitochondrial cristae induced *in vitro* by bee (*Apis mellifera*) venom and its derivatives, melittin and phospholipase A2, in isolated rat adrenocortical mitochondria



Adrian Florea^{a,*}, Andrei Patrick Varga^{a,b}, Horea Vlad Matei^a

^a Department of Cell and Molecular Biology, Faculty of Medicine, "Iuliu Hațieganu" University of Medicine and Pharmacy, 6 L. Pasteur St., 400349 Cluj-Napoca, Romania

^b Jibou County Hospital, 28 Libertatii St., 455200 Jibou, Romania

ARTICLE INFO

Keywords:
Isolated mitochondria
Adrenal cortex
Ultrastructure
Bee venom
Melittin
Phospholipase A2

ABSTRACT

We tested the ability of bee venom (BV), melittin (Mlt), and phospholipase A2 (PLA) – used in 5 concentrations each (5, 10, 15, 20 and 40 µg/100 µl) – to promote ultrastructural changes and reorganization of cristae *in vitro* in mitochondria isolated from rat adrenal cortex after a protocol optimized by us. Thus, apart from two control groups (CI and CS), in which the mitochondria were suspended into saline buffer and isolation medium respectively, 15 more groups of mitochondria were constituted, corresponding to the five different doses of the three substance tested (BV5 to M40; M5 to M40 and P5 to P40). The ultrastructural effects were quantified on transmission electron micrographs using a morphometry software. Values of 84.49 nm and 95.45 nm were calculated for median diameters of mitochondrial cristae in two control groups. Large and very large vesicular cristae, many with 2 or 3 membranes, were generated depending on dose among normal cristae in all treated groups. In the BV and Mlt treated groups, after an initial increase (up to 127.27 nm in V15 group and 151.2 nm in M10 group) due to stimulation of cristae fusion, the cristae diameter diminished as the doses increased, mainly by the collapse of the cristae. In the PLA treated groups, the cristae diameter increased continuously from 83.84 nm to 136.01 nm, by stimulated fusion of cristae, only the two largest doses promoting the collapse of cristae in some mitochondria. The highest percentage of abnormal cristae was found in the Mlt treated groups and next in BV treated groups. All substances tested produced pronounced ultrastructural variability of mitochondrial cristae *in vitro*: they also changed (depending on dose) mitochondrial shapes, generated matrix debris and the highest concentrations of BV and Mlt were responsible for mitochondrial breakdown. These ultrastructural alterations of mitochondrial crista in the presence of the BV molecules suggest a reduced capacity of adrenocortical mitochondria to synthesize steroid hormones consequently to BV envenomations and partially explain the toxic effects of the BV.

1. Introduction

It has been more than 60 years since the mitochondrial ultrastructure began to be elucidated. Palade and his co-workers reported the first isolation of intact mitochondria (Hogeboom et al., 1948), and later on he revealed the ultrastructure of this organelle on tissue ultrathin sections (Palade, 1952). Mitochondria were then isolated in order to elucidate their functions (Chance and Williams, 1955; Hackenbrock, 1966). Nowadays, mitochondrial dynamics (fissions and fusions, and continuous changes occurring inside this organelle, including at the level of cristae – Archer, 2013; Mishra et al., 2015; Mishra, 2016; Zick et al., 2009), and mitochondrial diseases (Debray et al., 2008; Mishra, 2016) are being considered as hot topics in the

study of mitochondria. These aspects are useful for both researchers and physicians, taking into account the major functions performed by mitochondria in cells (reviewed by Nunnari and Suomalainen, 2012).

Despite the fact that many scientists consider mitochondrial ultrastructure and physiology to be solved problems, they continue to draw attention. Thus, new and interesting data arise concerning diverse ultrastructural aspects of mitochondria from various organs and tissues in pathological conditions. On the other hand, due to their particular ultrastructure, mitochondria are regarded as a useful working tool in the basic research, in the study of various membrane-active molecules. In this respect, isolated mitochondria have been used as a valuable experimental model (Busquets et al., 2003; Krahnenbuhl et al., 1994). In addition, if liver isolated mitochondria have always been preferred (and

* Corresponding author.

E-mail addresses: aflorea@umfcluj.ro (A. Florea), dr.vargaandrei@gmail.com (A.P. Varga), hmatei@umfcluj.ro (H.V. Matei).

they still are), isolated mitochondria from nervous tissue (Dykens, 1994), kidney (Gross et al., 2011), or skeletal muscle (Kaufmann et al., 2006) were taken into consideration for research purposes.

Mitochondria from adrenocortical glands, particularly of *zona fasciculata* represent a special category. They share a common feature in animals and humans: their unique ultrastructure of cristae. Kadioglu and Harrison (1971), and Rhodin (1971) reported for the first time the presence of vesicular mitochondrial cristae in *zona fasciculata* of the adrenal glands. These vesicles were sized by O'Hare and Munro Neville (1973) who found a value of 60 nm for their diameter. Other studies, in which the actual ultrastructure of these cristae was investigated, showed that they were membranous tubules with bulbous tips and non-uniform diameter (Isola et al., 2010; Prince, 2002; Riva et al., 2003). The latter feature was given by deep constrictions placed at certain intervals along the tubular structures (Isola et al., 2010). Isola et al. (2010) also confirmed the diameter of around 60 nm for these mitochondrial cristae, and we reported a mean value of 58.5 nm for their diameter (Florea and Crăciun, 2011).

This pattern of adrenocortical mitochondrial cristae and implicitly the mitochondrial functions are disturbed in certain types of adrenal gland cancers: Snell adrenocortical carcinoma (Kimmel et al., 1974), in oncocytic adrenal cortical carcinoma (El-Naggar et al., 1991), in adrenocortical oncocytoma (Nguyen et al., 1992), and in genetic diseases such as: Zellweger syndrome (Baumgart et al., 2001), and adrenoleukodystrophy (McGuinness et al., 2003). Abnormal mitochondria have been also identified in experimental conditions, after exposure to hypoxia and Nandrolone (Koldysheva et al., 1999), after stimulation with ACTH (Merry, 1975), in *in vitro* transformed adrenocortical cells (Auersperg, 1978), and in mouse and chick embryo dying cells (Ba-Omar and Downie, 2006). In these circumstances, we believe that the particular ultrastructure of the adrenal gland mitochondria, as well as the high susceptibility of their numerous cristae to change in aspect and number in various conditions, recommend such mitochondria as an important experimental model in cell biology. Yet, despite their unique feature, the isolated adrenocortical mitochondria have rarely been used for *in vitro* studies. The reasons could be the reduced size of adrenal glands in experimental animals (mice, rats, guinea pigs) as well as technical difficulties allowing separation of only low amounts of these organelles.

Bee venom (BV) has been previously shown to have toxic effects on the adrenal gland mitochondria in mice (Pulido-Mendez et al., 2002; Rodriguez-Acosta et al., 2003); the researchers presented extensive destruction of cristae, but failed to provide further ultrastructural details.

We have a long-standing interest in studying the multiple physiological and ultrastructural effects of BV, and this study aimed to continue a previous one, in which we reported significant changes in the ultrastructure of mitochondrial cristae in the adrenocortical cells of rats induced *in vivo* consecutively to the BV injection (Florea and Crăciun, 2011). The BV used in very high doses (62 mg/kg) reorganized the cristae and resulted in formation of vesicular structures sometimes delimited by two or more concentric membranes. We concluded that BV could trigger those changes by a direct mechanism, involving the interaction of BV molecules. But, an indirect mechanism was taken into consideration, and discussed, involving BV interference with superior levels of the stress axis, also affected in identical experimental conditions, as shown earlier by us. In brain, the BV injected in single high doses severely damaged astrocytes and altered the ultrastructure of neurons surrounding the capillaries in the frontal cortex. It also generated epileptiform spike-wave complexes with increased frequency corresponding to neuronal hyperexcitation or irritation, and discharges of negative and biphasic sharp waves (Florea et al., 2011). In hypothalamus, the acute treatment with BV caused neuronal loss, again associated with cellular damages (Florea et al., 2009). At the level of the pituitary gland we found fewer secretion vesicles and with reduced density in corticotrope cells (responsible for secretion of

adrenocorticotropic hormone, controlling the activity of adrenocortical glands), along with extensive ultrastructural alterations (Florea et al., 2005). Thus, directly and/or indirectly, BV molecules could alter the ultrastructure of adrenocortical mitochondria, and implicitly their particular function, synthesis of steroid hormones in collaboration with the smooth endoplasmic reticulum. Therefore, in the bee venom envenomations, the reduced ability of reaction and defence of the stung victims' body (i.e. by disturbing eventually the adrenaline synthesis) should be also seriously taken into consideration.

The main objective of the present work was to investigate the ability of the crystallized whole BV to trigger directly ultrastructural changes of the mitochondrial cristae *in vitro*. Moreover, two BV derivatives, melittin (Mlt) and phospholipase A2 (PLA), were also used in our study in an attempt to elucidate the molecule(s) responsible for mitochondrial changes, and their mechanisms. In order to achieve these goals, we first isolated mitochondria from the rat adrenal cortex according to a protocol optimized by us. Then the isolated mitochondria were exposed to solutions of BV, Mlt and PLA of 5 different concentrations each, to investigate a potential dose-effect response. The effects upon the ultrastructure of mitochondrial cristae were quantitatively assessed on the transmission electron micrographs using a morphometry computer software.

Apart from Merry (1975) who previously reported the presence of "polylaminar mitochondria" in adrenal glands, suggesting that ACTH somehow induced formation of such abnormal cristae, there are no other studies showing such a dramatic reorganization of cristae. On this background, we consider our study will bring an important contribution to the field of cell biology, particularly to the study of biological membranes, by revealing the way into which membrane-active molecules from the bee venom interact with the mitochondrial cristae in the adrenocortical mitochondria.

2. Materials and methods

2.1. Animals and isolation of adrenocortical mitochondria

3-month old male Wistar rats (*Rattus norvegicus*) weighing 257.8 ± 18.4 g, grown in standardized condition, with no restriction to food, water and movement, were provided by the Animal Facility of "Iuliu Hațieganu" University of Medicine and Pharmacy, Cluj-Napoca, Romania. For ethical reasons, the minimum necessary number of rats was used in order to obtain adequate volumes of mitochondrial fractions. Experiments were performed twice using 6 animals each time, and handling of animals was performed according to a research protocol approved by the Ethic Commission of our university (No. 489/12.12.2011), in compliance with the rules of the National University Research Council and the European Communities Council Directive 86/609/EEC.

Mitochondria were isolated from epithelial cells of rat adrenal glands according to a protocol adapted after Brownie and Grant (1954); Frezza et al. (2007), and Petrescu and Tarba (1997). All rats were generally anaesthetized in an atmosphere of chloroform and killed by decapitation, and both adrenal glands were collected immediately from each animal. The glands trimmed from all fat (and medullar region removed) were transferred within several seconds into 6 ml of ice-cold mitochondria isolation medium consisting of 250 mM sucrose, 10 mM Tris-HCl at pH 7.4, and 0.1 mM ethylenediaminetetraacetic acid. Homogenization of the adrenal glands was performed for 45 s (20 passages) with a Nylon pestle in an AA Potter glass homogenizer (A.H. Thomas, Philadelphia, USA), at 1,350 rotations/min, and 0.5–1 °C (on ice). The homogenate was next subjected to differential centrifugation at 4 °C, using a Jouan CR-31 centrifuge (Jouan S.A., St. Herblain, France) as follows: centrifugation for 10 min at 600 g; 2) supernatant I was further centrifuged for 10 min at 7,000 g; supernatant II was removed and sediment II was re-suspended in fresh isolation medium and then centrifuged again for 10 min at 7,000 g. Supernatant III was

removed, and 400 µl sediment III (containing isolated mitochondria) were re-suspended in 1.3 ml fresh isolation medium (235 µl mitochondria/ml) and placed on ice.

2.2. Bee venom, melittin, phospholipase A2

Pure crystallized BV, collected by A.F. as previously described (Florea and Crăciun, 2011), was used in this study. Lyophilized Mlt from BV (product number M2272, m.w. 2,846.46 Da, purity 96%), and lyophilized PLA from BV (product number P9279, m.w. 14,500 Da, purity 1956.57 units/mg protein) were purchased from Sigma-Aldrich (St. Louis, USA). BV was kept at 4 °C, while Mlt and PLA were kept at –20 °C until use, according to producer's recommendations. In order to obtain aqueous solutions, BV, Mlt and PLA were reconstituted into an isotonic saline buffer consisting of 150 mM NaCl, 5.5 mM glucose and 5 mM 4-(2-hydroxyethyl)-1-piperazineethanesulfonic acid, at pH 7.4.

2.3. Experimental groups

Isolated mitochondria were added at 1-minute intervals in 3 ml plastic tubes with the different experimental solutions and the incubation was performed for 5 min at 0.5 °C (on ice). Two control groups of mitochondria were used in order to assess their ultrastructure in relation with the two different media used. In each tube of a first set, 100 µl of mitochondrial suspension was added to 100 µl of isolation medium for Control I (CI group). In a second set of tubes, 100 µl of mitochondrial suspension was added to 100 µl of saline buffer (the buffer used to reconstitute the BV, Mlt and PLA) for Control S (CS group). In a third set of tubes, 100 µl of mitochondrial suspension was added to 100 µl of BV solutions with different concentrations (5, 10, 15, 20 and 40 µg/100 µl). They were V groups: V5 to V40. In a fourth set of tubes, 100 µl of mitochondrial suspension was added to 100 µl of Mlt solutions of different concentrations (5, 10, 15, 20 and 40 µg/100 µl). These experimental groups were labeled M groups: M5 to M40. Finally, in a fifth set of tubes, 100 µl of mitochondrial suspension was added to 100 µl of PLA solutions of different concentrations (5, 10, 15, 20 and 40 µg/100 µl). These groups were labeled P groups: P5 to P40.

2.4. Transmission electron microscopy

The isolated adrenocortical mitochondria were processed for transmission electron microscopy (TEM) examination according to the usual protocols (Hagler, 2007; Watt, 2003). The 5-minute incubation of mitochondria with the different solutions was stopped with 1 ml of 2.7% glutaraldehyde (Electron Microscopy Sciences, Hatfield, USA) in 0.1 M phosphate buffer (pH 7.4), introduced in each tube for prefixation (1.5 h at 4 °C). The suspensions of mitochondria were next centrifuged for 10 min at 7,000 g, and then the pellets were washed with 0.1 M phosphate buffer (4 × 1 h). Postfixation was performed with 1 ml of 1.5% osmium tetroxide (Sigma-Aldrich, St. Louis, USA) in 0.15 M phosphate buffer (pH 7.4) (1.5 h at 4 °C). The postfixation was followed by washing in 200 µl 0.15 M phosphate buffer (pH 7.4) (2 × 1 h at 4 °C), the first one with re-suspension of the mitochondrial sediments, their transfer in embedding plastic capsules of 300 µl (EMS, Hatfield, USA), and another centrifugation for 10 min at 7,000 g at 4 °C. From that moment, the amount of every solution added over the mitochondrial pellets was of 200 µl for each capsule. The mitochondria were dehydrated through an acetone series, and embedded in Epon 812 resin (Fluka GmbH, Buchs Switzerland), after a previous infiltration through an acetone-epoxy series. The ultrathin sections of 60–80 nm thickness were cut with a DiATOME diamond knife (DiATOME, Hatfield, USA) using a Bromma 8800 ULTRATOME III ultramicrotome (LKB, Stockholm, Sweden), then collected on 300 mesh copper grids (Agar Scientific Ltd., Stansted, UK), and double contrasted with saturated (13%) alcoholic uranyl acetate (Merck, Darmstadt, Germany) and 2.8% lead citrate (Fluka GmbH, Buchs Switzerland). The examination of samples

was performed on a JEOL JEM 1010 transmission electron microscope (JEOL Ltd., Tokyo, Japan) at 80 kV. Images with prevalent orthodox mitochondria were captured using a Mega VIEW III camera (Olympus, Soft Imaging System, Münster, Germany).

2.5. Morphometric analysis

On the ultrathin sections obtained from all experimental groups, both orthodox and condensed mitochondria were observed but only the cristae in orthodox mitochondria were analyzed, for two reasons. On one hand, the condensed mitochondria (with electron dense matrix, and large intermembrane space) displayed cristae with a high variability (extremely diverse shapes and sizes), in all groups – including the control groups – and they could not provide relevant information. In addition, the ultrastructure of the orthodox mitochondria (with electron lucent matrix and narrow intermembrane space) resembles that of mitochondria *in vivo*. Thus, the changes in cristae shapes and sizes could be easily identified and analyzed, and also compared with those previously observed by us in the intact gland (Florea and Crăciun, 2011). On the TEM images, diameters of all visible cristae in the orthodox mitochondria were measured using CellID software (Olympus Soft Imaging Solutions GMBH, Münster, Germany). Since diameters up to 130 nm were found in the CI group, they were arbitrary considered by us as “normal values”, while cristae with larger diameters were regarded as “modified cristae”.

2.6. Statistical analysis

Means and standard deviations were calculated in order to compare our data with the literature data (Florea and Crăciun, 2011; Isola et al., 2010; O'Hare and Munro Neville, 1973). But, since the values of cristae diameters had a non normal distribution, in order to statistically analyze the results, medians and confidence intervals were calculated for each group (both for all cristae and modified cristae only). The median values were subjected to Kruskal-Wallis test (at confidence level of 99%, with a P value < 0.05 considered significant) and the results from the different groups were compared using Dunn's multiple comparison test. GraphPad Prism 5.00 (GraphPad Software Inc., La Jolla, USA) and Microsoft Excel (Microsoft Corporation, Redmond, USA) were used for the various parameters of the statistical analysis. Microsoft Excel was also used for graphical representation of the results.

3. Results

Due to the non normal distribution, median values of cristae diameters are presented in this section and discussed in Discussion section, while the mean values of cristae diameters are only briefly discussed.

3.1. Control groups

Round shaped orthodox mitochondria were observed in the both control groups (Fig. 1). In CI group, they displayed a high number of tubular cristae uniformly distributed within the matrix (Fig. 1A). The values for medians of cristae diameters are given in Table 1 and Fig. 2. In CS group, a slight tendency towards individual variability was noted when we examined the tubular cristae (Fig. 1B), and even cristae with diameter larger than 130 nm were found (Table 1). The medians calculated for all the cristae diameters in this group and for the modified cristae are also given in Table 1 and Fig. 2.

3.2. V groups

The orthodox mitochondria preserved a perfect round shape only in V5 group. Many of them also displayed the specific ultrastructure, with prevailing tubular cristae (Fig. 3A and B). In some mitochondria, a tendency of normal cristae to degenerate was observed (Fig. 3B and C).

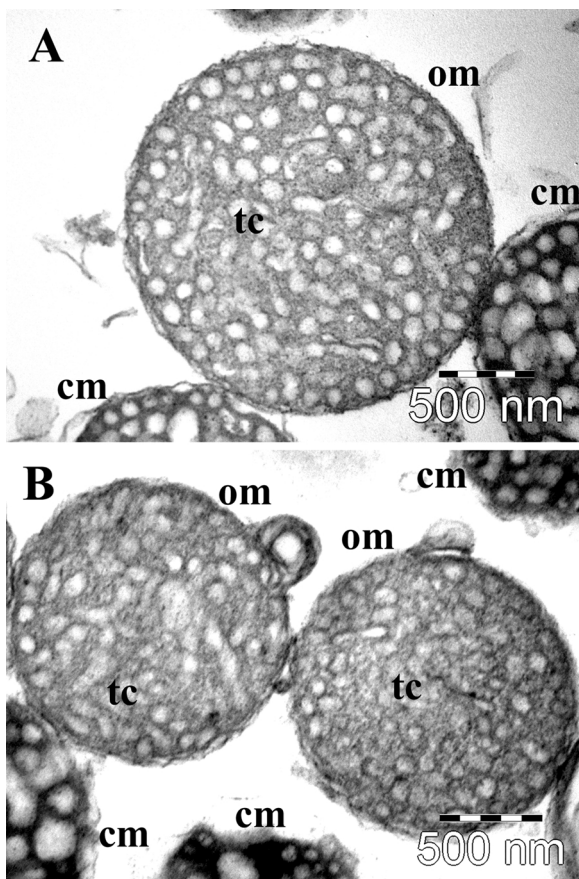


Fig. 1. TEM images presenting normal ultrastructure of adrenal gland mitochondria in CI group (A) and fine ultrastructural changes of adrenal gland mitochondria in CS (B), after a 5-min incubation of mitochondria with 100 μ l mitochondrial isolation medium (CI), and with 100 μ l saline buffer (CS) respectively; om, orthodox mitochondria; cm, condensed mitochondria; tc, tubular cristae.

However, mitochondria with modified cristae were also identified in this first experimental group (Fig. 3B and C). The modified cristae appeared mainly as vesicles with a single membrane, but abnormal cristae surrounded by two membranes were identified as well. Sometimes, the former vesicular cristae were pushed to periphery by the membrane of a very big crista (inset in Fig. 3C). In all the other V groups (V10-V40), mitochondria with irregular contour and even mitochondria with aberrant shapes were observed apart from the normal ones, and in increasing number with the used BV dose.

In V10 group, an accentuated disorganization of cristae was observed (Fig. 3D and E). The normal cristae were still present but they were fewer and smaller (Fig. 3E). On the other hand, this aspect was associated with the presence of more numerous and bigger vesicular cristae with 1–2 membranes (Fig. 3F). Moreover, in some mitochondria, such abnormal cristae occupied almost entirely the matrix

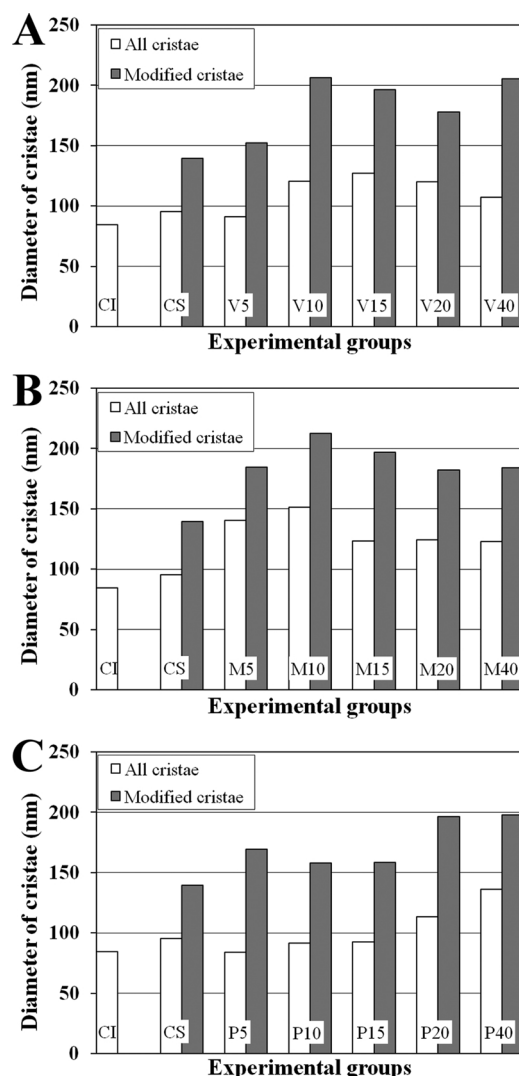


Fig. 2. Graphical representation of median values of mitochondrial cristae in the experimental groups of mitochondria: V groups, mitochondria incubated for 5 min with different doses of bee venom (A); M groups, mitochondria incubated for 5 min with different doses of melittin (B), and P groups, mitochondria incubated for 5 min with different doses of phospholipase A2 (C), as compared to the two control groups: CI (mitochondria suspended in isolation medium), and CS (mitochondria suspended in saline buffer). White bars: median diameter of all sized cristae; grey bars: median diameter of modified cristae.

(Fig. 3D), and in rare cases they generated unique structures with very large diameters (Fig. 3F).

In V15 group, mitochondria with normal cristae were still observed (Fig. 3G and H), but they also had modified (Fig. 3G) or even giant cristae (Fig. 3H). Many other orthodox mitochondria displayed a lower number of relatively large vesicular cristae with 1–3 membranes in the

Table 1

Diameters of mitochondrial cristae in Control groups, after a 5-min incubation of mitochondria with 100 μ l mitochondrial isolation medium (CI), and with 100 μ l saline buffer (CS).

Groups	All cristae					Modified cristae			
	median [#]	99% ci [#]	n	min [#]	max [#]	median [#]	99% ci [#]	n	%
CI	84.49	84.5-86.64	1155	48.44	129.15	-	-	-	-
CS	95.45*	96.69-99.68	1180	58.28	168.54	139.45	139.92-145.37	87	7.37

*statistical significant differences as compared to CI group (at $P < 0.0001$).

[#]values expressed in nm; ci-confidence interval; % -percentage of modified cristae.

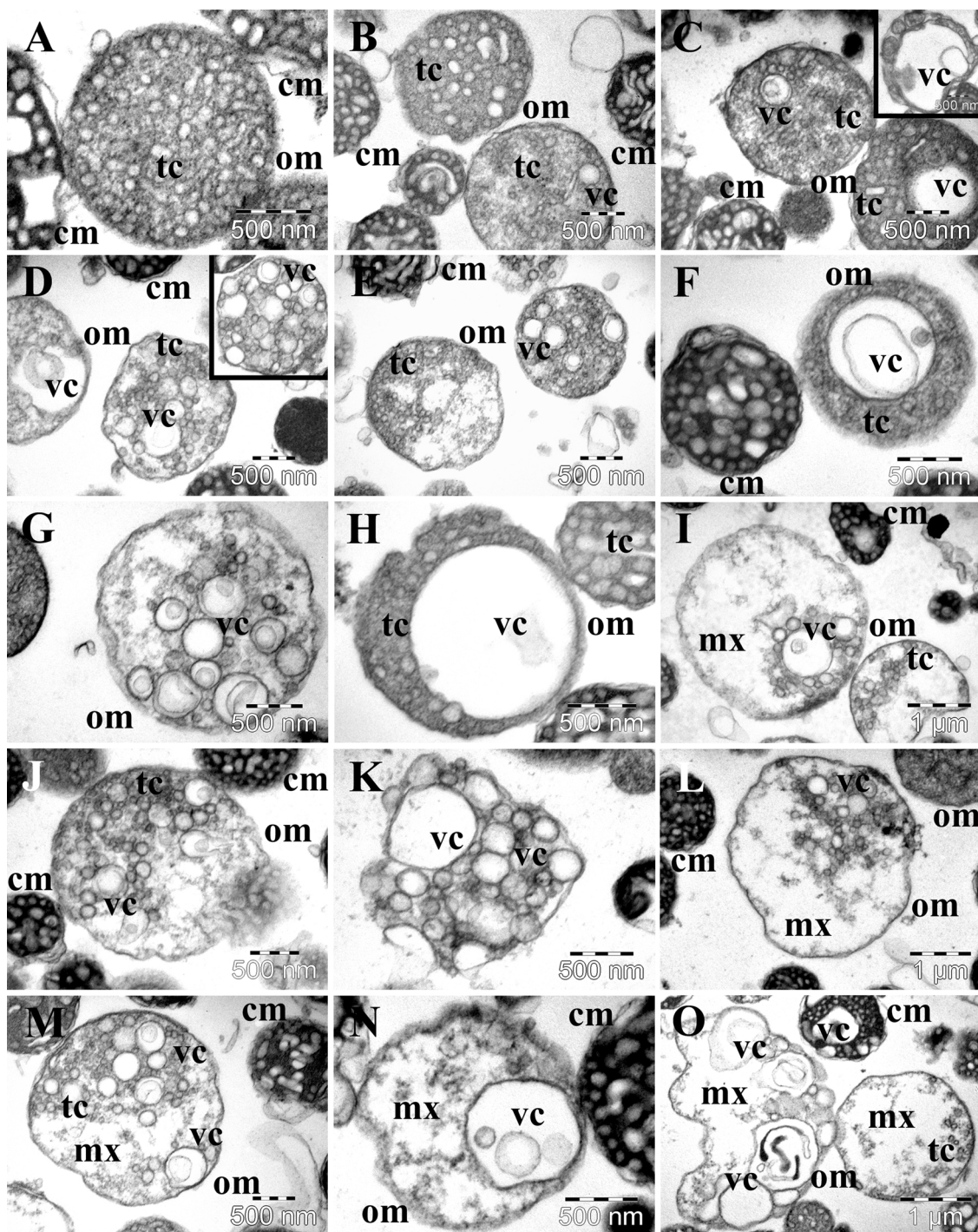


Fig. 3. TEM images presenting the most representative ultrastructural changes of orthodox adrenal gland mitochondria after a 5-min incubation of mitochondria with different doses of bee venom in V groups: V5 (A–C); V10 (D–F); V15 (G–I); V20 (J–L) and V40 (M–O). The first image from each row shows the prevalent ultrastructure of mitochondria in each group; the second image shows frequent aspects of mitochondria in each group; the third image shows rare ultrastructural changes found in each group; om, orthodox mitochondria; cm, condensed mitochondria; tc, tubular cristae; vc, vesicular cristae; mx, matrix.

matrix filled with debris (Fig. 3G). A few mitochondria contained only several cristae of different sizes grouped in a certain area within an electron transparent matrix (Fig. 3I).

In V20 group, most of the mitochondria had irregular shapes (Fig. 3J–L). They were filled with modified cristae (Fig. 3J and K) and debris (Fig. 3J), or showed a low number of abnormal cristae and electron transparent matrix (Fig. 3L). A particular ultrastructural aspect identified here was conversion between the two forms of mitochondria, orthodox and condensed (not shown), in which normal tubular cristae

could be observed.

In V40 group, all the orthodox mitochondria were deeply affected, presenting aberrant shapes, and matrix loaded with debris, or even being almost completely electron transparent (Fig. 3M–O). The orthodox mitochondria still contained a relative high number of cristae, especially of vesicular form, and with a wide range of diameters (Fig. 3M). Almost all orthodox mitochondria in this group had one or several very large vesicular cristae (Fig. 3M–O). Many mitochondria half-condensed and half-orthodox were observed in this group as well

Table 2

Diameters of mitochondrial cristae after a 5-min incubation of mitochondria with different doses of BV in V groups: V5, 5 µg BV/100 µl; V10, 10 µg BV/100 µl; V15, 15 µg BV/100 µl; V20, 20 µg BV/100 µl and V40, 40 µg BV/100 µl.

Groups	All cristae					Modified cristae			
	median [#]	99% ci [#]	n	min [#]	max [#]	median [#]	99% ci [#]	n	%
CS	95.45	96.69-99.68	1180	58.28	168.54	139.45	139.92-145.37	87	7.37
V5	91.05	97.45-110.6	998	47.14	2153.65	152.44*	159.33-242.81	136	13.63
V10	120.68*	150.69-168.13	1060	44.72	837.35	206.37*	229.92-258.11	470	44.34
V15	127.27*	153.21-169.86	1349	52.27	1333.94	196.58*	222.61-249.59	653	48.41
V20	119.99*	143.57-169.2	621	47.71	1243.31	177.69*	210.3-256.98	280	45.09
V40	107.36*	139.83-160.64	1060	36.45	1350.2	205.34*	231.84-271.82	423	39.91

*statistical significant differences as compared to CS group (at P < 0.0001).

#values expressed in nm; ci-confidence interval; %-percentage of modified cristae.

(not shown).

The medians calculated for all the cristae diameters in each V group are given in Table 2 and Fig. 2A, as well as the values for the modified cristae only. At P < 0.0001, the Dunn's test showed statistical significant differences when comparing the medians for cristae diameter in all the V groups with the values of the CS group. When we compared the medians of all cristae from the V groups with those from the CS group, only in V5 group the differences were non-significant. When the medians of only the modified cristae in the V groups were compared with those in the CS group, the differences were statistical significant in all cases (P < 0.0001). Analysis of the effects produced by the five BV doses showed significant differences in the median diameters of the cristae only when we compared the group V40 with either group V10, V15 or V20 (P < 0.0001), taking into account that the lowest values were recorded in the V5 and V40 groups, and the largest in the V15 group.

3.3. M groups

In M groups (Fig. 4), the orthodox mitochondria displayed various ultrastructural aspects beginning with the lowest concentration of Mlt. In the different M groups, not only cristae consisting of a single membrane were identified, but also cristae with 2–3 membranes.

In M5 group, most of the mitochondria displayed numerous modified cristae (Fig. 4A), while some of them were almost devoid of cristae on a background of rarefied matrix (not shown). A low number of mitochondria with prevailing normal ultrastructure of cristae was still found, but apart from the normal cristae, they also had a few abnormal vesicular cristae (Fig. 4B). A tendency for conversion of mitochondria from one form to the other was noted (Fig. 4C).

M10 group was characterised by an accentuated ultrastructural diversity of mitochondria. Mitochondrial variability was given both by their different shapes (Fig. 4E and F) and by their particular internal ultrastructure (Fig. 4D–F). Very few orthodox mitochondria maintained their normal aspect (not shown), while the majority displayed average degrees of ultrastructural alteration (Fig. 4D–F). The vesicular cristae with large diameters prevailed in such mitochondria. In some of these cristae, electron-dense inclusions were identified (Fig. 4D). The other ultrastructural extreme was represented by mitochondria with almost completely destroyed cristae (Fig. 4F), or even by complete broken mitochondria (not shown). In M10 group, condensed mitochondria also suffered deep changes (not shown).

Mitochondria in M15 group showed an accentuated ultrastructural variability, even if some orthodox mitochondria still had normal-looking cristae. However, most of the mitochondria in this group displayed various degrees of alteration, including irregular outline (Fig. 4G and H), modified cristae (Fig. 4G–I), aberrant shapes (Fig. 4I), or intermediate forms between condensed and orthodox mitochondria (Fig. 4H) – present in this group in the highest number. As in the previous groups, the presence of large or very large vesicular cristae was

accompanied by the presence of very small or normal cristae (Fig. 4G), and by a matrix loaded with debris (Fig. 4I).

In M20 group normal tubular cristae were still observed in rare orthodox mitochondria, but all such mitochondria also contained transformed cristae of different sizes (Fig. 4J–L), very large in some cases (Fig. 4L). It is important to note that very few mitochondria with rarefied matrix were found in this group (Fig. 4K), while the prevalent ones were those filled with large vesicular cristae (Fig. 4J). Intermediate mitochondria (orthodox-condensed) were observed here as well (not shown), with ultrastructural changes similar to those induced in the condensed mitochondria (not shown).

On the images obtained for M40 group, a much lower number of orthodox mitochondria was found as compared to the condensed form. Most of these mitochondria had rarefied, electron-transparent matrix, and a low number of small tubular cristae, large vesicular cristae (Fig. 4M–O), or even lamellar cristae (Fig. 4M). Orthodox mitochondria with very large vesicular cristae were in a very small ratio. As compared to M20 group, much more orthodox mitochondria with electron dense inclusions (or dense cristae) were observed here (not shown). An interesting ultrastructural aspect observed in the M40 group was a particular reaction of mitochondria to the high Mlt dose consisting in a rearrangement of cristae as vesicles in the intermembrane space. Some such mitochondria could have a granular, electron dense matrix, without cristae (Fig. 4N – inset), or a few tubular, small cristae (not shown). The Mlt highest dose influenced also the condensed mitochondria and the intermediate forms of mitochondria as well (not shown).

The medians calculated for the diameters of all cristae, and of the modified cristae, in each M group are presented in Table 3 and Fig. 2B. At P < 0.0001, the Dunn's test showed statistical significant differences when comparing the medians for cristae diameter in all the M groups with the values of the both control groups. When we compared the medians of the modified cristae in the M groups with those in the CS group, the differences were statistical significant in all cases (P < 0.0001). Analysis of the effects produced by the 5 Mlt doses showed significant differences in the median diameters of the cristae when we compared each of the groups M15, M20 and M40 with M5 (P < 0.0001), and each of the groups M15, M20 and M40 with M10 (P < 0.0001), taking into account that the largest value was recorded in M10 group, and the lowest in M40 group.

3.4. P groups

In P5 group, both round mitochondria and mitochondria with irregular outline were found. However, all of them contained vesicular abnormal cristae. Such altered cristae were either numerous and of various sizes, delimited by one membrane (Fig. 5A) or two membranes (Fig. 5B), or unique and very large, in mitochondria with relatively normal cristae (Fig. 5C).

Similar aspects were identified in P10 group (Fig. 5D–F), but here

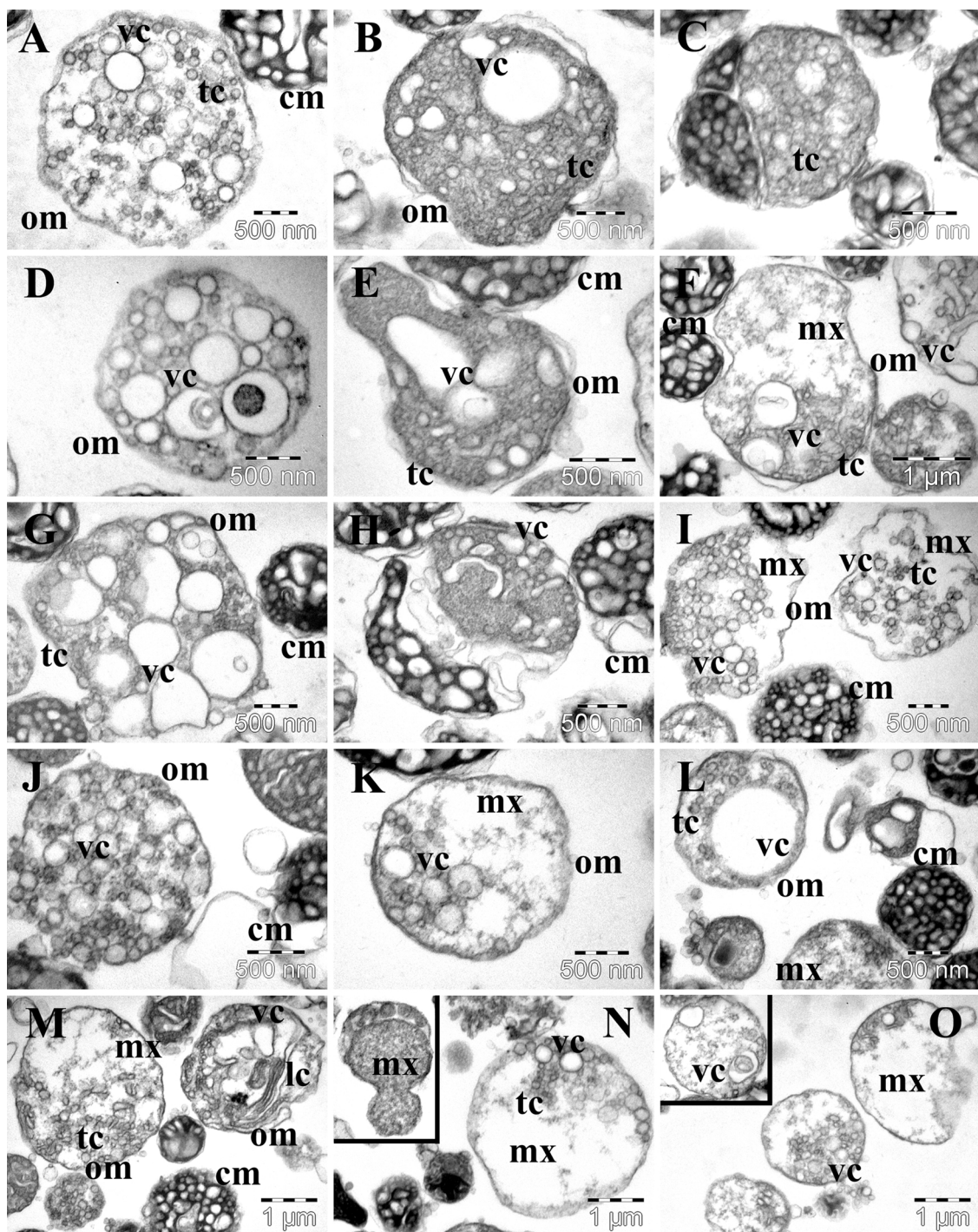


Fig. 4. TEM images presenting the most representative ultrastructural changes of orthodox adrenal gland mitochondria after a 5-min incubation of mitochondria with different doses of melittin in M groups: M5 (A–C); M10 (D–F); M15 (G–I); M20 (J–L) and M40 (M–O). The first image from each row shows the prevalent ultrastructure of mitochondria in each group; the second image shows frequent aspects of mitochondria in each group; the third image shows rare ultrastructural changes found in each group; om, orthodox mitochondria; cm, condensed mitochondria; tc, tubular cristae; lc, lamellar cristae; vc, vesicular cristae; mx, matrix.

the polymorphous mitochondria prevailed (Fig. 5D). Mitochondria with single, large vesicular cristae were in increased number in this group (Fig. 5E and F). On the other hand, almost all mitochondria also contained normal tubular cristae.

In P15 group (Fig. 5G–I) the majority of the mitochondria had round shapes or irregular contour, with normal cristae and a few vesicular ones (Fig. 5G), but also polymorphous mitochondria were in high number (Fig. 5H and I). Such mitochondria contained modified cristae displaying a wide range of shapes and sizes (Fig. 5H and I), many being

elongated and interconnected (Fig. 5I).

Mitochondria with high variability of shapes prevailed in P20 group (Fig. 5J–L). They contained inside either several modified, vesicular cristae (Fig. 5J and L), or only one, but bigger (Fig. 5K). Anyhow, small tubular cristae were still present (in low number) in mitochondria of this group. The general reduced number of cristae was associated with an electron transparent matrix of these mitochondria, and with the debris inside (Fig. 5L).

In P40 group, only rare orthodox mitochondria remained. Moreover,

Table 3

Diameters of mitochondrial cristae after a 5-min incubation of mitochondria with different doses of melittin in M groups: M5, 5 µg Mlt/100 µl; M10, 10 µg Mlt/100 µl; M15, 15 µg Mlt/100 µl; M20, 20 µg Mlt/100 µl and M40, µg Mlt/100 µl.

Groups	All cristae					Modified cristae			
	median [#]	99% ci [#]	n	min [*]	max [*]	median [*]	99% ci [*]	n	%
CS	95.45	96.69-99.68	1180	58.28	168.54	139.45	139.92-145.37	87	7.37
M5	140.38*	164.06-180.6	1345	57.48	1522.7	184.41*	215.07-239.65	761	56.58
M10	151.2*	177.73-194.18	1242	51.55	840.3	212.77*	232.86-253.95	747	60.15
M15	123.43*	156.09-173.88	1335	50.51	1165.17	196.94*	232.27-262.84	614	45.99
M20	124.24*	148.17-172.06	875	50.43	1704.45	182.25*	210.67-255.13	407	46.51
M40	122.93*	146.77-161.53	1356	36.45	1350.2	184.1*	209.16-234.19	632	46.61

*statistical significant differences as compared to CS group (at P < 0.0001).

[#]values expressed in nm; ci-confidence interval; %-percentage of modified cristae.

they were polymorphous (Fig. 5M-O), with aberrant shapes and very heterogeneous aspect of cristae and matrix. The modified cristae had different shapes and sizes, the largest ones containing inside other smaller vesicles (Fig. 5N and O). A high number of mitochondria had only a few tubular and vesicular cristae, and extended electron transparent areas in their matrix (Fig. 5O).

The medians of diameters of all cristae, as well as of the modified ones in each of the P groups are presented in Table 4 and Fig. 2C. At P < 0.0001, the Dunn's test showed statistical significant differences when the medians for cristae diameter in four of the P groups were compared with the values of the CI group, excepting the P5 group, in which the differences were non-significant. When we compared the data from P groups with those from CS group, the differences were non-significant in P5, P10, and P15 groups, and significant in P20 and P40 groups. When comparing the medians of the modified cristae in the P groups with those in the CS group, again at P < 0.0001, the differences were statistical significant in all cases. Analysis of the effects produced by the 5 PLA doses showed significant differences in the median diameters of the cristae when were compared all the P groups (P < 0.0001), excepting P10 versus P15. The lowest value was recorded in P5 group, and the largest in P40 group.

After comparison of median diameters of all cristae in the different groups on vertical line, according to dose, statistical significant differences were obtained for the groups V5, M5, P5, for the groups V10, M10, P10, and for the groups V40, M40, P40. For the other 6 groups, significant differences were found between V15 and P15 groups, and between M15 and P15 groups. No significant differences were found when data of the groups V20, M20, P20 were compared.

Another parameter taken into account in our study was the ratio of modified cristae among all the sized cristae. Tables 1–4 and Fig. 6 show percentage distribution of modified cristae in the different experimental groups. As compared with the low ratio of modified cristae observed in the CS group, the large cristae in the V groups were in increased number in the V5 to V15 groups (up to 48.41%), and thereafter their ratio decreased in the V20 group and even more in the V40 group (to 39.91%). Similarly, in M groups, an increase of large cristae ratio was observed in the M5 and M10 groups (but suddenly, reaching over 60% of all measured cristae), followed by the decrease of their ratio in the other M groups to a value of around 46%. Unlike in these two groups, the ratio of the large cristae in the P groups continuously increased depending on the PLA dose from 10.6% (in the P5 group) to 52.66% (in the P40 group).

4. Discussion

In this study, isolated mitochondria from the rat adrenocortical cortex were used as experimental model to demonstrate the ability of bee venom to change mitochondrial ultrastructure *in vitro*. Melittin and phospholipase A2, two important molecules purified from the BV, were tested as well in order to identify the mechanisms triggering the

ultrastructural changes. In all cases, the mitochondria were assessed both qualitatively and quantitatively. Our investigation was focused on isolated cortical adrenal mitochondria, suitable for a statistical analysis due to their particular ultrastructure. This is the main advantage emerging from the study of these mitochondria over mitochondria isolated from other organs.

It is well known that the method employed for isolation of mitochondria is critical for obtaining high quality organelles (Picard et al., 2011; Siess, 1983). In this context, perhaps the most difficult problem arising in the present study was separation of mitochondrial fraction. The protocol optimized by us allowed obtaining of pellets into which mitochondria from the *zona fasciculata* prevailed. It is very likely that *glomerulosa* and *reticularis* mitochondria also participated to formation of the pellets, but due to their reduced size, they sedimented in lower amounts at 7,000 g. However all the orthodox mitochondria observed on the sections, regardless their origin showed the particular pattern of cristae (tubular), similarly to those depicted in mitochondria *in situ* (Florea and Crăciun, 2011; Isola et al., 2010; Kadioglu and Harrison, 1971; Rhodin, 1971; Sekiyama and Yago, 1972). The high yield and purity of the mitochondrial fraction proved as well that our protocol was perfectly adequate. On the other hand, transmission electron microscopy is one of the very few methods of investigation sensitive enough to reveal and quantify the fine changes produced in mitochondria.

In order to quantify the effects of the three substances taken into account, two control groups were established. The mean diameters of cristae calculated by us for the control groups were higher as compared to the diameters of cristae *in situ*, on sections through the intact glands (see Introduction). This was a first interesting finding, reported here for the first time, as to the best of our knowledge. Moreover, mitochondria in the CS group (exposed for 5 min to the saline buffer prior to fixation) had a higher mean (and median) diameter of cristae than in the CI group (suspended in the isolation medium). The first difference was mainly due to the mechanical stress of homogenization. Then, the even larger cristae found in the CS group were also the result of the short time action of the saline buffer. This second finding is consistent with data reported by Hogeboom et al. (1948) who showed that isolated mitochondria could be deeply affected when released by homogenization into isotonic NaCl solution. But, an unexpected surprise arose when we found statistical significant differences between the median (and mean) diameters calculated for the two control groups.

Despite the fact that the saline medium was responsible for an increase of the cristae diameter, it is certainly evident that the presence of BV, Mlt and PLA was responsible for the important ultrastructural changes recorded by us in all experimental groups, which represented the main finding of the study. The statistically significant differences found in all experimental groups when compared to the control groups also confirmed the direct effects of the BV molecules. Initially it was a serious challenge to identify a pattern in the changes triggered by the various doses of BV, Mlt and PLA, but the problem was solved by analysing a high number of mitochondria in each group.

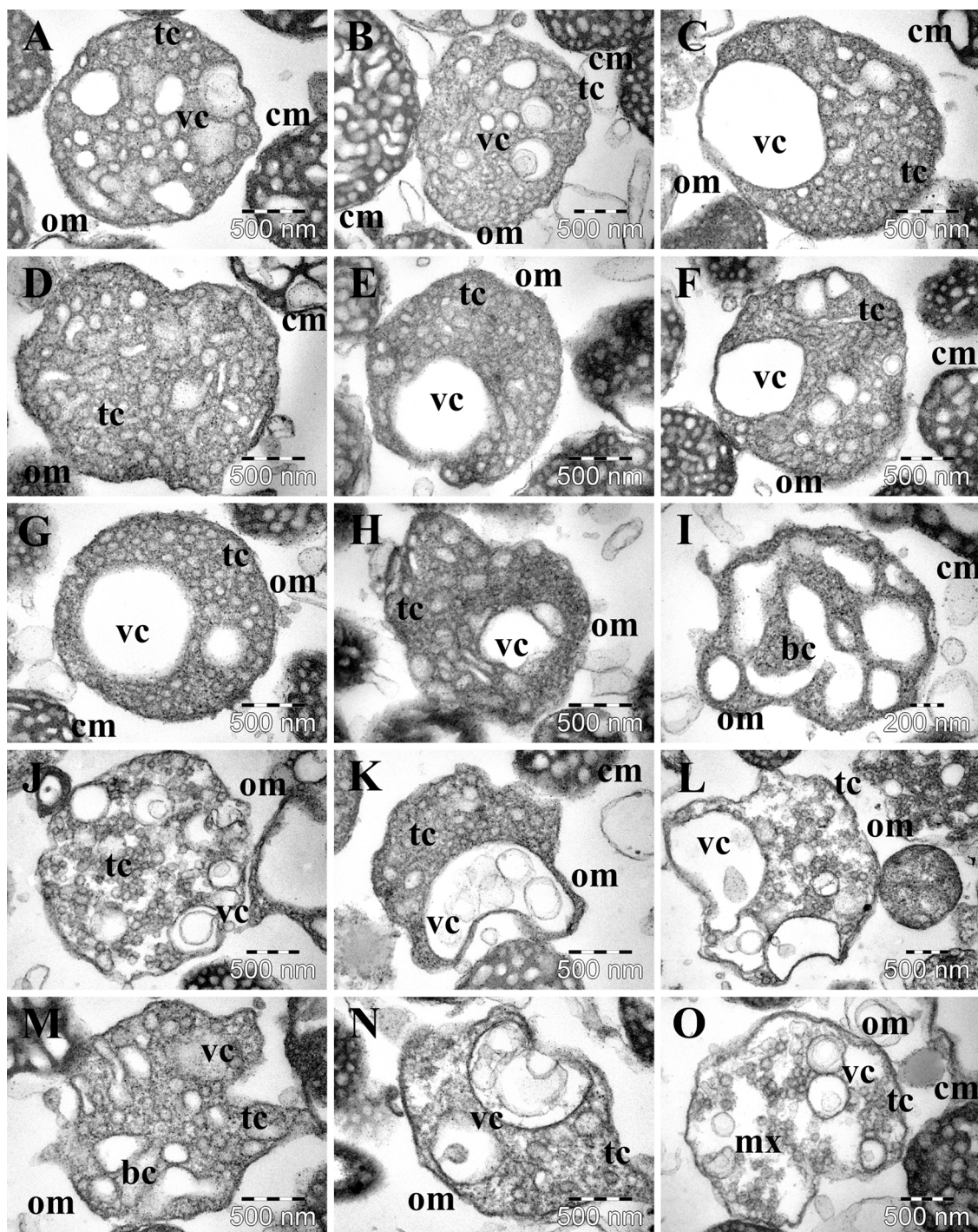


Fig. 5. TEM images presenting the most representative ultrastructural changes of orthodox adrenal gland mitochondria after a 5-min incubation of mitochondria with different doses of phospholipase A2 in P groups: P5 (A–C); P10 (D–F); P15 (G–I); P20 (J–L) and P40 (M–O). The first image from each row shows the prevalent ultrastructure of mitochondria in each group; the second image shows frequent aspects of mitochondria in each group; the third image shows rare ultrastructural changes found in each group; om, orthodox mitochondria; cm, condensed mitochondria; tc, tubular cristae; bc, bizarrely shaped cristae; vc, vesicular cristae; mx, matrix.

BV is known as a highly elaborated mixture of many organic and inorganic substances, most of them with pharmacological and toxicological relevance (Habermann, 1968, 1972; Neumann et al., 1952). Among these molecules, melittin and phospholipase A2 were of higher interest for us due to their high concentration into the dry venom, and to their ability to specifically interact with biological membranes. Mlt is a short peptide of 28 amino acids representing 40–50% of the dry BV (Banks and Shipolini, 1986; Habermann, 1972), and PLA is an enzyme

found in the BV in a concentration of 11–15% (Banks and Shipolini, 1986; Habermann, 1972; Schumacher et al., 1992). Both Mlt and PLA have high affinity for the cellular membranes, being able to disturb their structures and functions according to different molecular mechanisms.

Mlt, a cationic molecule, is one of the most used peptides in studies of lipid-protein interactions based on membrane models. Due to its amphiphilic nature, it is water soluble but also inserts in cell membranes as

Table 4

Diameters of mitochondrial cristae after a 5-min incubation of mitochondria with different doses of phospholipase A2 in P groups: P5, 5 µg PLA/100 µl; P10, 10 µg PLA/100 µl; P15, 15 µg PLA/100 µl; P20, 20 µg PLA/100 µl and P40, 40 µg PLA/100 µl.

Groups	All cristae					Modified cristae			
	median [#]	99% ci [#]	n	min [#]	max [#]	median [#]	99% ci [#]	n	%
CS	95.45	96.69–99.68	1180	58.28	168.54	139.45	139.92–145.37	87	7.37
P5	83.84	93.67–105.06	1592	40.61	1904.08	169.48	195.77–284.11*	169	10.62
P10	91.69	102.4–113.01	1212	43.11	1298.25	157.78	179.51–230.81*	195	16.09
P15	92.53	101.82–114.45	801	40.36	1219.81	158.53	167.49–221.92*	145	18.1
P20	113.62*	144.68–168.8	980	54.23	1978.14	169.63	225.82–278*	385	39.29
P40	136.01*	163.02–181.29	1090	57.29	1272.86	197.76	224.58–252.2*	574	52.66

*statistical significant differences as compared to CS group (at $P < 0.0001$).

#values expressed in nm; ci-confidence interval; %-percentage of modified cristae.

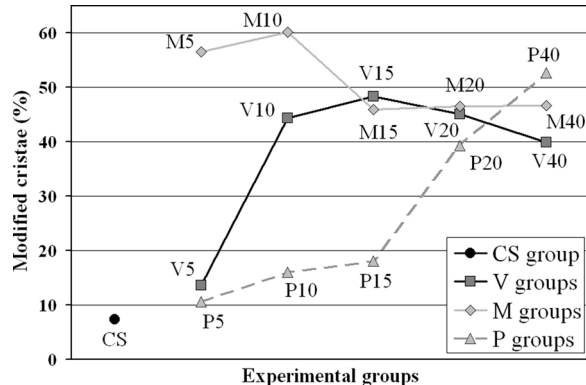


Fig. 6. Percentage distribution of modified cristae in the treated groups of mitochondria after a 5-min incubation: V groups (black line), M groups (grey line) and P groups (discontinued grey line), as compared to the control group CS (mitochondria suspended in saline buffer – black dot).

α -helix, and depending on concentration cancels their selective permeability for water molecules by formation of pores (Dempsey, 1990; Hristova et al., 2001; Ohki et al., 1994; Wimley and White, 2000). In most of the membranes, Mlt has pseudo-transmembrane orientation, but in cardiolipin-rich membranes (such as mitochondrial internal membranes) it also adopts a fully transmembrane orientation (Hung and Lee, 2006). At high concentrations Mlt may even trigger labilization of the phospholipid bilayer (Ladokhin and White, 2001). Mlt is small enough (2846.53 Da – Habermann, 1968; Terwilliger and Eisenberg, 1982a, b) to cross through porins and thus to interact with the both mitochondrial membranes. Even though Mlt has affinity for the both layers of a biological membrane, this molecule perturbs only the exposed layer of the membranes (Papo and Shai, 2003). It is worth pointing out this fact because as Mlt arrived in contact with mitochondria, and next inside the matrix in different concentrations (depending on the dose), it modified firstly the structure of the outer layer of the outer mitochondrial membrane, then modified both the inner layer of the outer membrane and the outer layer of the inner membrane, including of course the outer layer of cristae membrane. But unlike the inner membranes that were severely damaged, the outer mitochondrial membrane remained apparently intact, even at relative high concentrations of Mlt, due to its cholesterol content that prevented Mlt insertion in high amounts (Benachir et al., 1997). In addition, Mlt seems to have a similar sequence of amino acids with signal sequences of mitochondrial proteins imported from cytosol (Engelmann and Steitz, 1981; Von Heijne and Blomberg, 1979). This feature facilitated its interaction with mitochondrial membranes in our study, and possibly its transport into the matrix via specific transporters from the mitochondrial membranes.

PLA is a water soluble molecule that catalyzes the breakdown of membrane phospholipids (Habermann, 1972; Murakami and Kudo,

2002; Nicolas et al., 1997; Wilton and Waite, 2002), subsequently to its interfacial binding and formation of an α -helix in the N-terminal region (Berg et al., 2001; Burke and Dennis, 2009; Wilton and Waite, 2002). It appears that PLA does not fully integrate in the membrane (Lin et al., 1998), a docking model being proposed (Ahmed et al., 2000; Ball et al., 1999), and subsequent conformational changes allow the lytic activity (Ahmed et al., 1996). PLA contains two distinct domains oriented in the same direction: one for the substrate joining, and the catalytic domain surrounded by the first one (Berg et al., 2001; Lin et al., 1998). As a large and heavy molecule, it was not able to cross the outer membrane via porin in our experiments. This is why its action was firstly targeted against this membrane, and it arrived in contact with the cristae later and in lower amounts, only after the regional integrity of the outer membrane was compromised. Moreover, PLA interacts only with the outer monolayer of the membrane into which produces thus important conformational perturbations (Lin et al., 1998), an interesting aspect that could explain mitochondrial cristae fusions when such cristae with perturbed structure of the outer layer came in contact.

Altogether, these molecular mechanisms of interaction of Mlt and PLA with membranes were responsible for the ultrastructural changes produced *in vitro* in the isolated mitochondria. It is noteworthy that there are some striking differences between the results obtained in V and M groups as compared to those found in P groups. On one hand, the pattern of changes in the former groups was very similar, while the cristae in the latter suffered a different type of modification. The initial increase of cristae diameter followed the same pattern in the V and M groups (but more accelerated in the M groups) when the median diameter of all the cristae was considered. This increase resulted from generation of large vesicular cristae, by fusion of the tubular ones – phenomenon stimulated by the low BV and Mlt doses, and from disintegration of other cristae as well. Secondly, starting from a certain dose, the median diameter of mitochondrial cristae underwent a subsequent decrease (in inverse relation with the dose) in the V and M groups. This decrease was a consequence of cristae fragmentation and/or micellization. The evolution of median diameters of the modified cristae was almost identical in the V and M groups, the largest values being generated by the second doses of BV and Mlt. On the other hand, the enlargement of the cristae was continuous in the P groups, depending on dose, as the dose increased. This ultrastructural aspect of the modified cristae, different as compared to all the other groups, suggested a different mechanism involved in the cristae fusion. Also, while mitochondria with rarefied, electron transparent matrix were noted at low BV and especially Mlt concentrations, in the P groups only the highest dose of PLA induced this effect. Finally, we may assume that a certain number of mitochondria could be even more deeply affected or entirely broken apart under the effect of venom molecules and therefore they were not separated into the pellets obtained at 7,000 g.

The BV and especially Mlt inflow in large amounts also resulted in an irreversible collapse of the cristae. Concomitant with the disappearance of the cristae, an increased amount of debris was found in

the matrix. These observations are consistent with other reports (Dempsey, 1990; Dufourcq et al., 1986; Ohki et al., 1994) that described the ability of low doses of Mlt to rapidly disintegrate biological membranes with micellization of resulted phospholipids. In the P groups, this reaction of cristae micellization was rarely observed and delayed, being observed only at the largest doses.

However, formation of vesicular cristae is more difficult to be understood than fragmentation and collapse of the mitochondrial cristae, or disruption of the outer or both mitochondrial membranes, that can be easily explained by interactions of Mlt and PLA with the biological membranes. And yet, we previously described vesicular cristae formation in adrenal gland mitochondria *in vivo*, under the BV effect. According to our observations, that was a multistage process deployed during a longer time interval, and after a prior filtration and selective absorption of BV molecules in cells (Florea and Crăciun, 2011). Unlike the reaction of cristae to the very high BV dose in the intact adrenal gland, it seems that *in vitro* there was not a stable state of cristae; it is more appropriate to say that there was a continuous fusion of the small cristae, accompanied by their degradation. The ultrastructural changes of mitochondrial cristae included the presence of lamellar cristae. As compared to the observations of mitochondrial cristae alteration *in situ* under the influence of BV, in the current study the lamellar cristae were found only in a few mitochondria in the M40 group. As we postulated in our previous work, such lamellar cristae, that have been considered a normal and unique feature of mitochondria in the steroid-producing cells and not involved with ATP synthesis (Prince, 2002), could represent an intermediate form into formation of the larger cristae surrounded by two or more membranes (Florea and Crăciun, 2011). We also previously considered them as a first level of cristae alteration, which could be next, either destroyed, or closed into circular, concentric cristae. In the present study, their absence from almost all mitochondria could indicate their formation and/or disintegration very quickly within the 5 min of incubation, as well as an accelerated effect of BV molecules. For the fusion of the mitochondrial cristae their particular chemical composition should be taken into account, especially their high content of cardiolipin, a specific lipid molecule (diphosphatidylglycerol). It has been shown that in model membranes made of cardiolipin, melittin interacts *in vitro* with this phospholipid and triggers the formation of inverted phases (Batenburg et al., 1987), an essential aspect in the membrane fusions (Ellens et al., 1989). Cardiolipin is also known to participate in the shape of inner mitochondrial membranes, its reduction being associated with shape changes in the cristae (discussed in detail by Zick et al., 2009). Cristae reorganization was also reported consecutively to interaction of cardiolipin molecules with a truncated form (tBid) of a pro-apoptotic protein (Kim et al., 2004). We consider phospholipase A2 also possesses the ability to change the phospholipid composition of mitochondrial membranes, by reducing the cardiolipin content, thus participating in the cristae fusion. However, the detailed mechanisms of these interactions at molecular level are still to be elucidated with more sensitive methods.

In the present state of our knowledge, we consider the ultrastructural changes reported here as an unspecific way for mitochondria to respond by alterations to the chemical stress induced by the BV molecules. Such a view is in agreement with our previous work: we found abnormal cristae in mitochondria of other tissues after experimental exposure to BV (neurons – Florea et al., 2011, muscles – Florea and Crăciun, 2012; bone marrow, Florea and Crăciun, 2013). Unfortunately, we could not assess here mitochondrial functions by measuring the precise amount of consumed oxygen and produced ATP under the action of the toxic stressors used, further work being required to solve the interactions of venoms with the functional parameters of the adrenal glands mitochondria.

The presence of altered cristae in various types of cells as well as the general alteration of mitochondrial ultrastructure have important relevance at cellular level, interfering with various functions of the cells (Benard and Rossignol, 2008; Kasahara and Scorrano, 2014; Picard

et al., 2016). Changes occurred in the mitochondrial ultrastructure have been also related to severe mitochondrial dysfunctions in different pathological conditions (Ba-Omar and Downie, 2006; Ghadially, 1985, 1988; Griparic and van der Bliek, 2001), consecutive to experimental treatments with toxins that inhibited mitochondrial activity (Shah et al., 1982), or during the induced cell death by necrosis (Ardisson-Araújo et al., 2013). Functional alteration of mitochondria in diseases has been often associated with hypertrophied or bizarrely-shaped cristae, or with the presence of paracrystalline inclusions within the matrix (Debray et al., 2008). Furthermore, abnormal mitochondrial ultrastructure has been reported in different types of cells in patients suffering from mitochondrial genetic diseases. Gilchrist et al., 1996 reported abnormal mitochondrial cristae in neurons in MELAS syndrome. Abnormal cristae were also observed in muscle cells, in dilated cardiomyopathy (Arbuscini et al., 1998), in Kearns-Sayre syndrome (Schwartzkopff et al., 1988), and in MEHMO syndrome (Leshinsky-Silver et al., 2002). Cristae remodeling is also a feature of mitochondria during the apoptosis (Frezza et al., 2006).

5. Conclusions

We optimized an efficient method of separation of adrenal gland mitochondria with high yield, and the results presented here showed that these mitochondria represented a valuable experimental model, which, along with the investigation methods used were perfectly adequate for achieving the main goal of the study. We proved the ability of crystallized whole bee venom to trigger directly ultrastructural changes of the mitochondrial cristae *in vitro*. Moreover, we also proved that either of the two important molecules of the BV, Mlt and PLA tested alone was able to produce ultrastructural changes of the mitochondria, but according to different molecular mechanisms, since the changes were different.

The complex modifications of mitochondria *in vitro* were largely similar to those occurred *in vivo* in the adrenal glands under the influence of BV molecules. BV, as well as Mlt and PLA altered mitochondrial ultrastructure, especially of the cristae. We found here a continuous, dose-dependent transformation of cristae from their normal, tubular ultrastructure to large vesicles surrounded by one or several overlaid membranes, and eventually to their complete collapse. On the other hand, all three membrane-active agents used by us in the present study possessed the ability to turn the mitochondria from one form to the other (orthodox to condensed, or vice-versa). This ability was higher for Mlt.

Knowing and understanding the molecular mechanisms involved in the alteration of mitochondrial ultrastructure under the action of BV could be useful in the accidental envenomation of animals and humans. Our results also demonstrate the importance of looking at mitochondrial changes (particularly of adrenocortical mitochondria) in a larger context of using such molecules as tools to study the interactions of cationic peptides or enzymes with the membranes.

Funding

This work was supported by the “Iuliu Hațieganu” University of Medicine and Pharmacy, Cluj-Napoca, Romania [grant number 27020/49/2011 awarded to AF] from which melittin and phospholipase A2 were purchased.

Conflict of interest

None.

Acknowledgments

Thanks are due to Mr. Savian Cruceru, who kindly let us to collect the bee venom in his apiary.

References

- Ahmed, T., Kelly, S.M., Lawrence, A.J., Mezna, M., Price, N.C., 1996. Conformational changes associated with activation of bee venom phospholipase A2. *J. Biochem.* 120, 1224–1231.
- Ahmed, T., Kelly, S.M., Price, N.C., Lawrence, A.J., 2000. Activation of phospholipase A₂ by long chain fatty acyl groups involves a novel unstable linkage. *J. Biochem.* 127, 871–875.
- Arbustini, E., Diegoli, M., Fasani, R., Grasso, M., Morbini, P., Banchieri, N., Bellini, O., Dal Bello, B., Pilotto, A., Magrini, G., Campana, C., Fortina, P., Gavazzi, A., Narula, J., Vigano, M., 1998. Mitochondrial DNA mutations and mitochondrial abnormalities in dilated cardiomyopathy. *Am. J. Pathol.* 153 (5), 1501–1510.
- Archer, S.L., 2013. Mitochondrial dynamics – mitochondrial fission and fusion in human diseases. *N. Engl. J. Med.* 369 (23), 2236–2251. <http://dx.doi.org/10.1056/NEJMra1215233>.
- Ardisson-Araújo, D.M.P., Morgado, F.D.S., Schwartz, E.F., Corzo, G., Ribeiro, B.M., 2013. A new theraphosid spider toxin causes early insect cell death by necrosis when expressed *in vitro* during recombinant baculovirus infection. *PLoS One* 8 (12), e84404. <http://dx.doi.org/10.1371/journal.pone.0084404>.
- Auersperg, N., 1978. Effects of culture conditions on the growth and differentiation of transformed rat adrenocortical cells. *Cancer Res.* 38, 1872–1884.
- Banks, B.E.C., Shipolini, R.A., 1986. Chemistry and pharmacology of honeybee venom. In: Piek, T. (Ed.), *Venoms of the Hymenoptera: Biochemical, Pharmacological and Behavioural Aspects*. Academic Press, Orlando, pp. 329–416.
- Ba-Omar, T.A., Downie, J.R., 2006. Microscopic study of cell death in the adrenal glands of mouse and chick embryos. *Tissue Cell* 38 (4), 243–250. <http://dx.doi.org/10.1016/j.tice.2006.05.001>.
- Batenburg, A.M., Hibbeln, J.C.L., Verkleij, A.J., de Kruijff, B., 1987. Melittin induces H₁ phase formation in cardiolipin model membranes. *Biochim. Biophys. Acta* 903 (1), 142–154.
- Baumgart, E., Vanhorebeek, I., Grabenbauer, M., Borgers, M., Declercq, P.E., Fahimi, H.D., Baes, M., 2001. Mitochondrial alterations caused by defective peroxisomal biogenesis in a mouse model for Zellweger syndrome (PEX5 knockout mouse). *Am. J. Pathol.* 159 (4), 1477–1494. [http://dx.doi.org/10.1016/S0002-9440\(10\)62534-5](http://dx.doi.org/10.1016/S0002-9440(10)62534-5).
- Benachir, T., Monette, M., Grenier, J., Lafleur, M., 1997. Melittin-induced leakage from phosphatidylcholine vesicles is modulated by cholesterol: a property used for membrane targeting. *Eur. Biophys. J.* 25, 201–210.
- Benard, G., Rossignol, R., 2008. Ultrastructure of the mitochondrion and its bearing on function and bioenergetics. *Antioxid. Redox Signal.* 10 (8), 1313–1342. <http://dx.doi.org/10.1089/ars.2007.2000>.
- Berg, O.G., Gelb, M.H., Tsai, M.D., Jain, M.K., 2001. Interfacial enzymology: the secreted phospholipase A2-paradigm. *Chem. Rev.* 101 (9), 2613–2653. <http://dx.doi.org/10.1021/cr990139w>.
- Brownie, A.C., Grant, J.K., 1954. The *in vitro* enzymic hydroxylation of steroid hormones. I. Factors influencing the enzymic 11β-hydroxylation of 11-deoxycorticosterone. *Biochem. J.* 57 (2), 255–263.
- Burke, J.E., Dennis, E.A., 2009. Phospholipase A2 structure/function, mechanism, and signaling. *J. Lipid Res.* 50 (Suppl), S237–S242. <http://dx.doi.org/10.1194/jlr.R800033-JLR200>.
- Busquets, S., Aranda, X., Ribas-Carbo, M., Azcon-Bieto, J., Lopez-Soriano, F.J., Argiles, J.M., 2003. Tumour necrosis factor-alpha uncouples respiration in isolated rat mitochondria. *Cytokine* 22 (1–2), 1–4.
- Chance, B., Williams, G.R., 1955. Respiratory enzymes in oxidative phosphorylation. II. The steady state. *J. Biol. Chem.* 217 (1), 409–427.
- Debray, F.G., Lambert, M., Mitchell, G.A., 2008. Disorders of mitochondrial function. *Curr. Opin. Pediatr.* 20 (4), 471–482. <http://dx.doi.org/10.1097/MOP.0b013e328306eb66>.
- Dempsey, C.E., 1990. The action of melittin on membranes. *Biochim. Biophys. Acta* 1031 (2), 143–161.
- Dufourcq, J., Faucon, J.F., Fourche, G., Dasseux, J.L., Le Maire, M., Gulik-Krzywicki, T., 1986. Morphological changes of phosphatidylcholine bilayers induced by melittin: vesicularization, fusion, discoidal particles. *Biochim. Biophys. Acta* 859 (1), 33–48. [http://dx.doi.org/10.1016/0005-2736\(86\)90315-9](http://dx.doi.org/10.1016/0005-2736(86)90315-9).
- Dykens, J.A., 1994. Isolated cerebral and cerebellar mitochondria produce free radicals when exposed to elevated Ca²⁺ and Na⁺: implications for neurodegeneration. *J. Neurochem.* 63 (2), 584–591.
- Ellens, H., Siegel, D.P., Alford, D., Yeagle, P.L., Boni, L., Lis, L.J., Quinn, P.J., Bentz, J., 1989. Membrane fusion and inverted phases. *Biochemistry* 28 (9), 3692–3703.
- El-Naggar, A.K., Evans, D.B., MacKay, B., 1991. Oncocytic adrenal cortical carcinoma. *Ultrastruct. Pathol.* 15 (4–5), 549–556.
- Engelmann, D.M., Steitz, T.A., 1981. The spontaneous insertion of proteins into and across membranes: the helical hairpin hypothesis. *Cell* 23 (2), 411–422.
- Florea, A., Crăciun, C., 2011. Abnormal mitochondrial cristae were experimentally generated by high doses of *Apis mellifera* venom in the rat adrenal cortex. *Micron* 42 (5), 434–442. <http://dx.doi.org/10.1016/j.micron.2010.12.006>.
- Florea, A., Crăciun, C., 2012. Bee (*Apis mellifera*) venom produced toxic effects of higher amplitude in rat thoracic aorta than in skeletal muscle – an ultrastructural study. *Microsc. Microanal.* 18 (2), 304–316. <http://dx.doi.org/10.1017/S1431927611012876>.
- Florea, A., Crăciun, C., 2013. Bee venom induced *in vivo* ultrastructural reactions of cells involved in the bone marrow erythropoiesis and of circulating red blood cells. *Microsc. Microanal.* 19 (2), 393–405. <http://dx.doi.org/10.1017/S1431927612014195>.
- Florea, A., Oprea, M.C., Crăciun, C., Puică, C., 2005. Reacții ale celulelor somatotrope, corticotrope și gonadotrope adenohipofizare la administrarea veninului de albine în două variante experimentale. *Ann. Soc. Natl. Biol. Cell* 10, 223–234.
- Florea, A., Puică, C., Crăciun, C., 2009. Reactions of rat hypothalamus to very high doses of bee venom. An histologic and ultrastructural study. *Annals R.S.C.B.* 14 (2), 109–117.
- Florea, A., Puică, C., Vințan, M., Benga, I., Crăciun, C., 2011. Electrophysiological and structural aspects in the frontal cortex after the bee (*Apis mellifera*) venom experimental treatment. *Cell. Mol. Neurobiol.* 31 (5), 701–714. <http://dx.doi.org/10.1007/s10571-011-9667-4>.
- Frezza, C., Cipolat, S., Martins de Brito, O., Micaroni, M., Beznousenko, G.V., Rudka, T., Bartoli, D., Polishuck, R.S., Danial, N.N., De Strooper, B., Scorrano, L., 2006. OPA1 controls apoptotic cristae remodeling independently from mitochondrial fusion. *Cell* 126 (1), 177–189. <http://dx.doi.org/10.1016/j.cell.2006.06.025>.
- Frezza, C., Cipolat, S., Scorrano, L., 2007. Organelle isolation: functional mitochondria from mouse liver, muscle and cultured fibroblasts. *Nat. Protoc.* 2 (2), 287–295. <http://dx.doi.org/10.1038/nprot.2006.478>.
- Ghadially, F.N., 1985. *Diagnostic Electron Microscopy of Tumours*, second ed. Butterworths, London.
- Ghadially, F.N., 1988. *Ultrastructural Pathology of the Cell and Matrix*. Butterworth-Heinemann, Boston.
- Gilchrist, J.M., Sikirica, M., Stopa, E., Shanske, S., 1996. Adult-onset MELAS evidence for involvement of neurons as well as cerebral vasculature in strokelike episodes. *Stroke* 27 (8), 1420–1423.
- Gripaios, L., van der Bliek, A.M., 2001. The many shapes of mitochondrial membranes. *Traffic* 2 (4), 235–244.
- Gross, V.S., Greenberg, H.K., Baranov, S.V., Carlson, G.M., Stavrovskaya, I.G., Lazarev, A.V., Kristal, B.S., 2011. Isolation of functional mitochondria from rat kidney and skeletal muscle without manual homogenization. *Anal. Biochem.* 418 (2), 213–223. <http://dx.doi.org/10.1016/j.ab.2011.07.017>.
- Habermann, E., 1968. *Chimie, pharmacologie et toxicologie du venin*. In: Chauvin, R. (Ed.), *Traité de Biologie de l'abeille*, pp. 363–387 Masson, Paris.
- Habermann, E., 1972. Bee and wasp venoms. The biochemistry and pharmacology of their peptides and enzymes are reviewed. *Science* 177 (4046), 314–322.
- Hackenbrock, C.R., 1966. Ultrastructural bases for metabolically linked mechanical activity in mitochondria. *J. Cell Biol.* 30 (2), 269–297.
- Hagler, H.K., 2007. Ultramicrotomy for biological electron microscopy. In: Kuo, J. (Ed.), *Electron Microscopy: Methods and Protocols*, second ed. Humana Press, Totowa, New York, pp. 67–96.
- Hogeboom, G.H., Schneider, W.C., Palade, G.E., 1948. Cytochemical studies of mammalian tissue. I. Isolation of intact mitochondria from rat liver; some biochemical properties of mitochondria and submicroscopic particulate material. *J. Biol. Chem.* 172 (2), 619–638.
- Hristova, K., Dempsey, C.E., White, S.H., 2001. Structure, location, and lipid perturbations of melittin at the membrane interface. *Biophys. J.* 80 (2), 801–811. [http://dx.doi.org/10.1016/S0006-3495\(01\)76059-6](http://dx.doi.org/10.1016/S0006-3495(01)76059-6).
- Hung, W.C., Lee, M.T., 2006. The interaction of melittin with *E. coli* membrane: the role of cardiolipin. *Chin. J. Phys.* 44, 137–149.
- Isola, R., Solinas, P., Loy, F., Mariotti, S., Riva, A., 2010. 3-D structure of mitochondrial cristae in rat adrenal cortex varies after acute stimulation with ACTH and CRH. *Mitochondrion* 10 (5), 472–478. <http://dx.doi.org/10.1016/j.mito.2010.05.007>.
- Kadioglu, D., Harrison, R.G., 1971. The functional relationships of mitochondria in the rat adrenal cortex. *J. Anat.* 110 (Pt 2), 283–296.
- Kasahara, A., Scorrano, L., 2014. Mitochondria: from cell death executioners to regulators of cell differentiation. *Trends Cell Biol.* 24 (12), 761–770. <http://dx.doi.org/10.1016/j.tcb.2014.08.005>.
- Kaufmann, P., Torok, M., Zahno, A., Waldhauser, K.M., Brecht, K., Krahenbuhl, S., 2006. Toxicity of statins on rat skeletal muscle mitochondria. *Cell. Mol. Life Sci.* 63 (19–20), 2415–2425. <http://dx.doi.org/10.1007/s00108-006-6235-z>.
- Kim, T.H., Zhao, Y., Ding, W.X., Shin, J.N., He, X., Seo, Y.W., Chen, J., Rabinowich, H., Amoscato, A.A., Yin, X.M., 2004. Bid-cardiolipin interaction at mitochondrial contact site contributes to mitochondrial cristae reorganization and cytochrome C release. *Mol. Biol. Cell.* 15, 3061–3072.
- Kimmel, G.L., Peron, F.G., Haksar, A., Bedigian, E., Robidoux Jr, W.F., Lin, M.T., 1974. Ultrastructure, steroidogenic potential, and energy metabolism of the Snell adrenocortical carcinoma 494. A comparison with normal adrenocortical tissue. *J. Cell Biol.* 62 (1), 152–163.
- Koldysheva, E.V., Lushnikova, E.L., Proskuryakova, I.S., 1999. Ultrastructural reorganization of adrenal cortex in rats exposed to hypoxia and treated with Nandrolone. *Bull. Exp. Biol. Med.* 127 (5), 535–539.
- Krahenbuhl, S., Talos, C., Fischer, S., Reichen, J., 1994. Toxicity of bile acids on the electron transport chain of isolated rat liver mitochondria. *Hepatology* 19 (2), 471–479.
- Ladokhin, A.S., White, S.H., 2001. 'Detergent-like' permeabilization of anionic lipid vesicles by melittin. *Biochim. Biophys. Acta* 1514 (2), 253–260.
- Leshinsky-Silver, E., Zinger, A., Bibi, C.N., Barash, V., Sadeh, M., Lev, D., Sagiv, T.L., 2002. MEHMO (mental retardation, epileptic seizures, hypogenitalism, microcephaly, obesity): a new X-linked mitochondrial disorder. *Eur. J. Hum. Genet.* 10 (4), 226–230. <http://dx.doi.org/10.1038/sj.ejhg.5200791>.
- Lin, Y., Nielsen, R., Murray, D., Hubbell, W.L., Mailer, C., Robinson, B.H., Gelb, M.H., 1998. Docking phospholipase A2 on membranes using electrostatic potential-modulated spin relaxation magnetic resonance. *Science* 279 (5358), 1925–1929.
- McGuiness, M.C., Lu, J.F., Zhang, H.P., Dong, G.X., Heinzer, A.K., Watkins, P.A., Powers, J., Smith, K.D., 2003. Role of ALDP (ABCD1) and mitochondria in X-linked adrenoleukodystrophy. *Mol. Cell. Biol.* 23 (2), 744–753.
- Merry, B.J., 1975. Mitochondrial structure in the rat adrenal cortex. *J. Anat.* 119 (3), 611–618.
- Mishra, P., 2016. Interfaces between mitochondrial dynamics and disease. *Cell Calcium*

- 60 (3), 190–198. <http://dx.doi.org/10.1016/j.cea.2016.05.004>.
- Mishra, P., Varuzhanian, G., Pham, A.H., Chan, D.C., 2015. Mitochondrial dynamics is a distinguishing feature of skeletal muscle fiber types and regulates organellar compartmentalization. *Cell Metab.* 22 (6), 1033–1044. <http://dx.doi.org/10.1016/j.cmet.2015.09.027>.
- Murakami, M., Kudo, I., 2002. Phospholipase A2. *J. Biochem.* 131 (3), 285–292.
- Neumann, W., Habermann, E., Amend, G., 1952. Zur papierelektrophoretischen fraktionierung tierischer gifte. *Die Naturwissenschaften* 39 (12), 286–287.
- Nguyen, G.K., Vriend, R., Ronaghan, D., Lakey, W.H., 1992. Heterotopic adrenocortical oncocytoma. A case report with light and electron microscopic studies. *Cancer* 70 (11), 2681–2684.
- Nicolas, J.P., Lin, Y., Lambeau, G., Ghomashchi, F., Lazdunski, M., Gelb, M.H., 1997. Localization of structural elements of bee venom phospholipase A2 involved in N-type receptor binding and neurotoxicity. *J. Biol. Chem.* 272 (11), 7173–7181.
- Nunnari, J., Suomalainen, A., 2012. Mitochondria: in sickness and in health. *Cell* 148 (6), 1145–1159. <http://dx.doi.org/10.1016/j.cell.2012.02.035>.
- O'Hare, M.J., Munro Neville, A., 1973. Morphological responses to corticotrophin and cyclic AMP by adult rat adrenocortical cells in monolayer culture. *J. Endocrinol.* 56 (3), 529–536.
- Ohki, S., Marcus, E., Sukumaran, D.K., Arnold, K., 1994. Interaction of melittin with lipid membranes. *Biochim. Biophys. Acta* 1194 (2), 223–232. [http://dx.doi.org/10.1016/0005-2736\(94\)90303-4](http://dx.doi.org/10.1016/0005-2736(94)90303-4).
- Palade, G., 1952. The fine structure of mitochondria. *Anat. Rec.* 114 (3), 427–451.
- Papo, N., Shai, Y., 2003. Exploring peptide membrane interaction using surface Plasmon resonance: differentiation between pore formation versus membrane disruption by lytic peptides. *Biochemistry* 42 (2), 458–466. <http://dx.doi.org/10.1021/bi0267846>.
- Petrescu, I., Tarba, C., 1997. Uncoupling effects of diclofenac and aspirin in the perfused liver and isolated hepatic mitochondria of rat. *Biochim. Biophys. Acta* 1318 (3), 385–394. [http://dx.doi.org/10.1016/S0005-2728\(96\)00109-0](http://dx.doi.org/10.1016/S0005-2728(96)00109-0).
- Picard, M., Taivassalo, T., Gouspillou, G., Hepple, R.T., 2011. Mitochondria: isolation, structure and function. *J. Physiol.* 589 (Pt 18), 4413–4421. <http://dx.doi.org/10.1113/jphysiol.2011.212712>.
- Picard, M., Wallace, D.C., Burelle, Y., 2016. The rise of mitochondria in medicine. *Mitochondrion* 30, 105–116. <http://dx.doi.org/10.1016/j.mito.2016.07.003>.
- Prince, F.P., 2002. Lamellar and tubular associations of the mitochondrial cristae: unique forms of the cristae present in steroid-producing cells. *Mitochondrion* 1 (4), 381–389.
- Pulido-Mendez, M., Rodriguez-Acosta, A., Finol, H.J., 2002. Adrenal cortex ultrastructural alterations caused by zootoxins. *Microsc. Microanal.* 8 (9S2), 926CD–927CD 10.1017.S1431927602107318.
- Rhodin, J.A., 1971. The ultrastructure of the adrenal cortex of the rat under normal and experimental conditions. *J. Ultrastruct. Res.* 34 (1), 23–71.
- Riva, A., Loffredo, F., Ucccheddu, A., Testa Riva, F., Tandler, B., 2003. Mitochondria of human adrenal cortex have tubular cristae with bulbous tips. *J. Clin. Endocrinol. Metab.* 88 (4), 1903–1906. <http://dx.doi.org/10.1210/jc.2002-030013>.
- Rodriguez-Acosta, A., Vega, J., Finol, H.J., Pulido-Mendez, M., 2003. Ultrastructural alterations in cortex of adrenal gland caused by the toxic effect of bee (*Apis mellifera*) venom. *J. Submicros. Cytol. Pathol.* 35 (3), 309–314.
- Schumacher, M.J., Schmidt, J.O., Egen, N.B., Dillon, K.A., 1992. Biochemical variability of venoms from individual European and Africanized honey bees. *J. Allergy Clin. Immunol.* 90 (1), 59–65.
- Schwartzkopff, B., Frenzel, H., Breithardt, G., Deckert, M., Losse, B., Toyka, K.V., Borggreve, M., Hort, W., 1988. Ultrastructural findings in endomyocardial biopsy of patients with Kearns-Sayre syndrome. *J. Am. Coll. Cardiol.* 12 (6), 1522–1528.
- Sekiya, S., Yago, N., 1972. A study on the correlation between function and ultrastructure in the rat adrenal cortex. *Acta Pathol. Jpn.* 22, 77–98.
- Shah, A.J., Sahgal, V., Muschler, G., Subramani, V., Singh, H., 1982. Morphogenesis of the mitochondrial alterations in muscle diseases. *J. Neurol. Sci.* 55 (1), 25–37.
- Siess, E.A., 1983. Influence of isolation media on the preservation of mitochondrial functions. *Hoppe Seylers Z. Physiol. Chem.* 364 (3), 279–289.
- Terwilliger, T.C., Eisenberg, D., 1982a. The structure of melittin. I. Structure determination and partial refinement. *J. Biol. Chem.* 257 (11), 6010–6015.
- Terwilliger, T.C., Eisenberg, D., 1982b. The structure of melittin. II. Interpretation of the structure. *J. Biol. Chem.* 257 (11), 6016–6022.
- Von Heijne, G., Blomberg, C., 1979. Trans-membrane translocation of proteins. *Eur. J. Biochem.* 97 (1), 175–181.
- Watt, I.M., 2003. The Principles and Practice of Electron Microscopy. Cambridge University Press, Cambridge.
- Wilton, D.C., Waite, M., 2002. Phospholipases. In: Vance, D.E., Vance, J.E. (Eds.). *Biochemistry of Lipids, Lipoproteins and Membranes*, fourth ed. Elsevier Science, Oxford, pp. 291–314.
- Wimley, C.W., White, S.H., 2000. Determining the membrane topology of peptides by fluorescence quenching. *Biochemistry* 39 (1), 161–170.
- Zick, M., Rabl, R., Reichert, A.S., 2009. Cristae formation – linking ultrastructure and function of mitochondria. *Biochim. Biophys. Acta* 1793 (1), 5–19. <http://dx.doi.org/10.1016/j.bbamcr.2008.06.013>.